Supplementary Material and Methods

Mouse husbandry

Conditional *Ctnnb1* loss-of-function mutant mice (*Ctnnb1*$^{LacZ/fl}$;*Col10a1*-Cre^{+} = *Ctnnb1*^{LOFHTC}) were generated by intercrossing *Ctnnb1*$^{fl/fl}$ females with males double heterozygous for *Ctnnb1* LacZ knock-in null (Huelsken et al., 2000) and BAC-Col10a1-Cre (*Col10a1*-Cre, #1465 and #1421) transgenic alleles (Gebhard et al., 2008). Conditional *Ctnnb1* gain-of-function mutant mice (*Ctnnb1*$^{ex3fl/+}$;*Col10a1*-Cre^{+} = *Ctnnb1*^{GOFHTC}) were generated by intercrossing females homozygous for the *Ctnnb1* exon3 floxed allele (Harada et al., 1999) with *Col10a1*-Cre (#1465 and #1421) heterozygous males.

For genetic restoration experiments, either females double-homozygous for *Opg/Tnfrsf11b* knock-out (Mizuno et al., 1998) and *Ctnnb1* exon3 floxed alleles were crossed with males double-heterozygous for the *Opg* knock-out and Col10-Cre transgenic alleles, or males double-homozygous for the floxed *Rankl/Tnfsf11* (Xiong et al., 2011) and *Ctnnb1* alleles were crossed to *Rankl*$^{fl/+}$;*Ctnnb1*$^{LacZ/+}$;*Col10a1*-Cre^{+} females. Homozygous *Opg* (Mizuno et al., 1998) and *Rank/Tnfrsf11a*$^{\Delta/\Delta}$ (Hanada et al., 2009) mutants were generated by the intercrossing of heterozygous animals, conditional *Rankl* mutants by the intercrossing of *Rankl*$^{fl/fl}$ males with *Rankl*$^{fl/+}$;*Col10a1*-Cre^{+} females.

For quantitative gene expression analysis in sorted HTCs and for the transdifferentiation assays, the following crosses were set up: for conditional *Ctnnb1*^{LOFHTC} embryos, males double heterozygous for *Ctnnb1* LacZ-null and *Col10a1*-Cre alleles were crossed with females double-homozygous for Rosa26-EYFP (Srinivas et al., 2001) and *Ctnnb1* floxed alleles. For controls and

Ctnnb1^{GOFHTC} embryos, males heterozygous for the *Col10a1*-Cre transgenic allele were crossed with females homozygous for the Rosa26-EYFP transgene or with females double homozygous for the Rosa26-EYFP transgene and the *Ctnnb1* exon3 floxed allele, respectively.

Microcomputed tomography (microCT) and histomorphometric analysis

Scanning was carried out at 40 kV, 600 µA, w/o filter, 0.5° rotation steps, an image pixel size of 8.52 µm and an exposure set to 525 ms. Reconstruction of sections was carried out with software associated with the scanner (Nrecon v1.6.9.8) with beam hardening correction set to 40%. Analysis of trabeculae in P28 specimens was carried out using the CT Analyzer v1.13.11.0 software, at a region from 852.35 µm to 1707.7 µm from the growth plate.

Processing of specimens

For histology, immunohistochemistry, and immunofluorescent stainings, the limbs of embryos, newborn (P0) and three-day-old (P3) specimens were fixed in 4% paraformaldehyde at 4°C overnight, dehydrated and embedded in paraffin. Bones obtained from four-week-old mice (P28) were fixed for 24 h in 4% paraformaldehyde at 4°C and embedded in paraffin or methyl methacrylate (MMA) (Technovit 9100, Heraeus Kulzer GmbH, Germany). For paraffin embedding, bones were decalcified for one week in 0.5 M EDTA pH 8.0 and dehydrated into xylene. For MMA embedding, fixed bones were washed overnight in PBS containing 10% sucrose, dehydrated (2 days 70% ethanol, 2 days 95% ethanol, twice for 1 day 2-propanol, twice for 2 days xylene) and embedded in methyl methacrylate (MMA).

Histology

For histological stainings sections were deparaffinized and rehydrated into H_2O. For alcian blue / von Kossa staining mineralized tissue was stained by incubation of sections in 2% silver-nitrate solution under light exposure (60W bulb) for 1 h, washed with 1% acetic acid and subsequently stained for 15 min in alcian blue staining solution (20 mg alcian blue in 70 ml EtOH, 30 ml acetic acid), tissue was counterstained with eosin, dehydrated and mounted with DPX (Sigma). Alcian blue / eosin staining was performed in principle as described above, omitting the incubation step in silver-nitrate solution. For hematoxylin and eosin (H&E) staining sections were incubated in Mayer's Haemalaun (Waldeck GmbH & Co. KG, Divison Chroma) for 5 min, washed in running tap water, counterstained with an alcoholic solution of eosin Y (Sigma) for 45 sec, dehydrated and mounted with DPX. For von Kossa / toluidine blue staining on 5 µm MMA sections, sections were deplasticized (two times 20 min xylene, 20 min 2-methoxyethyl acetate, 10 min acetone), rehydrated into H_2O and processed as following: sections were stained in 2% silver-nitrate solution under light exposure for 1 h, washed with distilled water, incubated in toluidine blue solution (0.1% toluidine blue O and 0.1% sodium tetraborate in H_2O) for 30 sec, dehydrated and mounted with DPX (Sigma). For tartrate-resistant acid phosphatase (TRAP) staining, rehydrated sections were incubated for 1 h at 37°C in freshly prepared TRAP staining solution: buffer (40 mM sodium acetate and 10 mM sodium tartrate, pH 5.0) containing 0.1 mg/ml naphtol AS-MX phosphate disodium salt (Sigma) and 0.6 mg/ml fast red violet LB salt (Sigma). Sections were washed with distilled water, counterstained for 1 min with Mayer's Haemalaun, washed in running tap water and mounted with Faramount (Dako).

Immunohistochemistry and Immunofluorescence

For immunohistochemical stainings deparaffinized and rehydrated sections were treated with 3% H_2O_2 for 30 min and blocked with appropriate 10% blocking serum for 30 min. Antigen retrieval was achieved by incubating sections in 10 mM sodium citrate (pH 6.0) at 95°C for 20 min for β-catenin, by proteinase K treatment 40 µg/ml for 15 min at 37°C, followed by 10 min at RT for CD31/PECAM-1, and by using chondroitinase ABC (Sigma, #C3667, 2 mU/ml in PBS (pH 8.0)) at 37°C for 2 h for the aggrecan neoepitope DIPEN. No antigen retrieval was required for Opg, Osterix and Sox9. Incubation with the respective primary antibodies was performed either for 1 h at room temperature or overnight at 4°C: mouse anti-β-catenin (1:200, BD Transduction Laboratories, #610154), rat anti-mouse CD31 (1:25, BD Pharmingen, #550274), rabbit anti-mouse DIPEN (1:1000, clone BC4, a gift from Professor Amanda Fosang, University of Melbourne, Australia), biotinylated goat anti-mouse OPG/TNFRSF11B (15µg/ml, R&D systems, #BAF459), rabbit anti-mouse Sp7/Osterix (1:500, Abcam, #ab22552) and rabbit anti-mouse Sox9 (1:1000, Millipore, #AB5535). Sections were subsequently incubated with the appropriate biotinylated secondary antibody (Vector Laboratories) for 1 hour at room temperature followed by color development with the Vectastain Elite ABC Kit (Vector Laboratories) and DAB substrate (Sigma). For Osterix and Sox9, HRP-conjugated secondary antibodies were used (Promega). Immunostaining for Collagen type II was performed with a mouse anti-chicken Col II antibody (1:25, Chemicon, #MAB8887) using the Dako ARK Peroxidase kit for Mouse Primary Antibodies (Dako, #K3954) according to the manufacturer's instructions. Antigen retrieval for Col II was achieved by incubating sections with 5 µg/ml proteinase type XXIV (Sigma, #P8038) for 10 min at 37°C followed by 10 µg/ml hyaluronidase type 1-S (Sigma, #H3506) for

30 min at 37°C. For double immunofluorescence, sections were incubated with rabbit anti-mouse Sp7/Osterix (1:250, Abcam, #ab22552), rabbit anti-mouse Runx2 (1:50, Abcam, #ab23981), rabbit anti-mouse Sox9 (1:1000, Millipore, #AB5535), rabbit anti-human Ki67 (1:1000, Novocastra Laboratories, #NCL-Ki67p), rabbit anti-mouse Cleaved Caspase-3 (Asp175) (1:20, Cell Signaling, #9661) or rabbit anti-mouse FABP4 (1:500, Abcam, #ab13979). Previous heat-mediated antigen retrieval was achieved by incubation in 10 mM sodium citrate (pH 6.0) at 95°C for 20 min for Runx2, Ki67 and FABP4, and by Tris/EDTA-Buffer (pH 9.0) at 95°C for 15 min for cleaved Caspase-3. To detect TUNEL-positive cells sections were pretreated for 15 min at 37°C with 20 µg/ml proteinase K in 10 mM Tris/HCl, pH 7.5. TUNEL assay was performed using the *In situ* Cell Death Detection Kit from Roche (Roche, #11684795910) according to the manufacturer's instructions. After visualization of the first primary antibody with Alexa Fluor 568 goat anti-rabbit IgG (Molecular Probes), sections were incubated with chicken anti-mouse GFP (1:500, Abcam, #ab13970) or rat anti-mouse Endomucin (1:50, Santa Cruz, #sc-65495) followed by detection with Alexa Fluor 488 goat anti-chicken IgG or Alexa Fluor 488 goat anti-rat IgG (Molecular Probes). Nuclei were counterstained with DAPI. Antibody specificity was confirmed using the respective IgG or IgY isotype control antibodies.

RNA isolation from FACS sorted primary HTCs and total skeletal elements

E16.5 or P0 limbs were dissected in PBS and isolated skeletal elements were sequentially digested with 0.3% Trypsin (Invitrogen, GIBCO, #15090-046) for 30 min at 37℃, washed with culture medium (DMEM/F12, 10% FCS), followed by digestion with 0.1% collagenase type 1-S (Sigma, # C1639) for 3 h at 37℃ in a bacterial dish in a tissue culture incubator, while separating the cells every hour by

pipetting. For RNA-isolation from whole P0 skeletal elements, cells were collected, washed twice with PBS, filtered through a cell strainer and cell pellets were stored at -80°C until RNA isolation. For cell sorting of YFP positive cells from E16.5 skeletal elements, fresh culture medium was added and the cells were incubated overnight. Prior to cell sorting, cells were washed with PBS/2% FCS, debris was removed using a cell strainer and the cell suspension was subjected to FACS sorting for transgenic, endogenous YFP fluorescence by the staff of the BioOptics unit of the IMP (Vienna) using a FACS Aria III (BD Biosciences, Franklin Lakes, New Jersey, USA). FACS sorted E16.5 hypertrophic cells were washed twice with PBS and either frozen or directly processed. Total RNA was extracted from the respective cell pellets using the RNeasy Micro Kit (Qiagen, #74004) or RNeasy Mini Kit (Qiagen, #74106) according to the manufacturer's instructions, including a DNase I treatment. RNA concentration was determined by OD measurement on a nano-drop 2000 (Thermo Scientific, Waltham, Massachusetts, USA) or a BioPhotometer plus (Eppendorf AG, Hamburg, Germany).

cDNA synthesis

For first-strand cDNA synthesis, 1 µg of total RNA from FACS sorted primary material was reverse transcribed by using Oligo(dT)$_{12-18}$ and SuperScript II Reverse Transcriptase (Invitrogen, #18064-022). Reverse transcriptase was inactivated at 70°C for 15 min and RNA in RNA:DNA duplex was digested by incubation with RNaseH (Roche, #10786357001) for 20 min at 37°C. A total of 500 ng RNA from whole P0 skeletal elements was reverse transcribed using PrimeScript RT reagent Kit (Perfect Real Time) (TaKaRa, #RR037A) with oligo dT primer. For quantitative RT-PCR, cDNA was diluted 1 in 10 with distilled water.

Real-time PCR analysis

2 µl of 1 in 10 diluted 1st strand cDNA of the RNA from E16.5 sorted chondrocytes were mixed with Fast Start SBG master mix (Roche, #04673484001) in a total reaction volume of 25 µl and quantitative PCR was performed using the Bio-Rad CFX96 cycler. Reaction conditions were 95°C 10 min, 45x (95°C 15 sec, 60°C 30 sec, 72°C 30 sec), 72°C 5 min, plate read at 80°C, melting curve: from 55°C to 99°C, in 0.5°C increments for 5 sec + plate read. For the RNA from whole P0 skeletal elements SYBR Premix Ex Taq II (Tli RNaseH Plus) (TaKaRa, #RR820Q) and 3 µl of 1 in 10 diluted cDNA in a final volume of 25 µl were used. Gene expression was monitored using a BioRad CFX96 cycler and following protocol: 95°C 30 sec, 45x (95°C 15 sec, 60°C 30 sec, 72°C 20 sec + plate read), 95°C 10 sec, melting curve: 55°C to 99°C, in 0.5°C increments for 5 sec + plate read. For quantitative real-time PCR, each reaction was performed in at least in duplicate and repeated using independent sample sets. Products were analyzed by agarose gel electrophoresis and melting curves. Values were calculated using the comparative ΔC(t) method and normalized to the expression levels of housekeeping genes (*Hprt* for sorted HTCs and *Hprt*, *Actb* for whole skeletal elements). For primer sequences, product size, and Genbank accession number see Table S1.

Gene	Sequence	Product size (bp)	GenBank Access No.
Mmp13	5’-TTCTGGTCTTCTGGCACACGCTTT-3’ 5’-CCAAGCTCATGGGCAGCAACAATA-3’	132	NM_008607
Vegf	5’-AAGGAGAGCAGAAGTCCCATGA-3’ 5’-CTCAATTGGACGGCAGTAGCT-3’	74	NM_009505
Sox9	5’-AACAAGCCACACGTCAAGC-3’ 5’-AAGGGTCTCTTCTCGCTCTC-3’	161	NM_011448
Ihh	5’-AGCGCTTCAAAGAGCTCACC-3’ 5’-CCATCTTCATCCCAGCCTTC-3’	184	NM_010544
Opg	5’-GAAGCCACGCAAAAGTGTGG-3’ 5’-CTACACTCTCGGCATTCACTTTGG-3’	145	NM_008764
Opg*	5’-CCAAGAGCCCAGTGTTTCTT-3’ 5’-CCAAGCCAGCCATTGTTAAT-3’	115	NM_008764
Rankl	5’-GGCCACAGCGCTTCTCAG-3’ 5’-GAGTGACTTTATGGGAACCCGAT-3’	144	NM_011613
Rankl*	5’-CCAAGATCTCTAACATGACG -3’ 5’-CACCATCAGCTGAAGATAGT -3’	139	NM_011613
Opn	5’-CCCATCTCAGAAGCAGAATCTCC-3’ 5’-TTCATCCGAGTCCACAGAATCC-3’	187	NM_009263
Opn*	5’-GATGATGATGACGATGGAGACC-3’ 5’-CGACTGTAGGGACGATTGGAG-3’	147	NM_009263
ChM-I	5’-TCCTTGAACTCTGTGGCGACCT-3’ 5’-GAGCACTGTTTCTCACGACTTC-3’	99	NM_010701
Timp-1	5’-CTATAGTGCTGGCTGTGGGGTGTG-3’ 5’-TTCCGTGGCAGGCAAGCAAAGT-3’	150	NM_011593
Timp-2	5’-CCAGAAGAAGAGCCTGAACCA-3’ 5’-GTCCATCCAGAGGCACTCATC-3’	112	NM_011594
Timp-3	5’-GGCCTCAATTACCGCTACCA-3’ 5’-CTGATAGCCAGGGTACCCAAAA-3’	135	NM_011595
Hprt	5’-AGCTACTGTAATGATCAGTCAACG-3’ 5’-AGAGGTCCTTTTCACCAGCA-3’	198	NM_013556
Actb	5’-TTGCTGACAGGATGCAGAAGGAGA-3’ 5’-ACTCCTGCTTGCTGATCCACATCT-3’	159	NM_007393

Table S1. Primer sequences for PCR

All primers span exon-intron boundaries with the exception of primers marked with an asterisk used for amplification on YFP-sorted E16.5 material.

Supplementary Figures

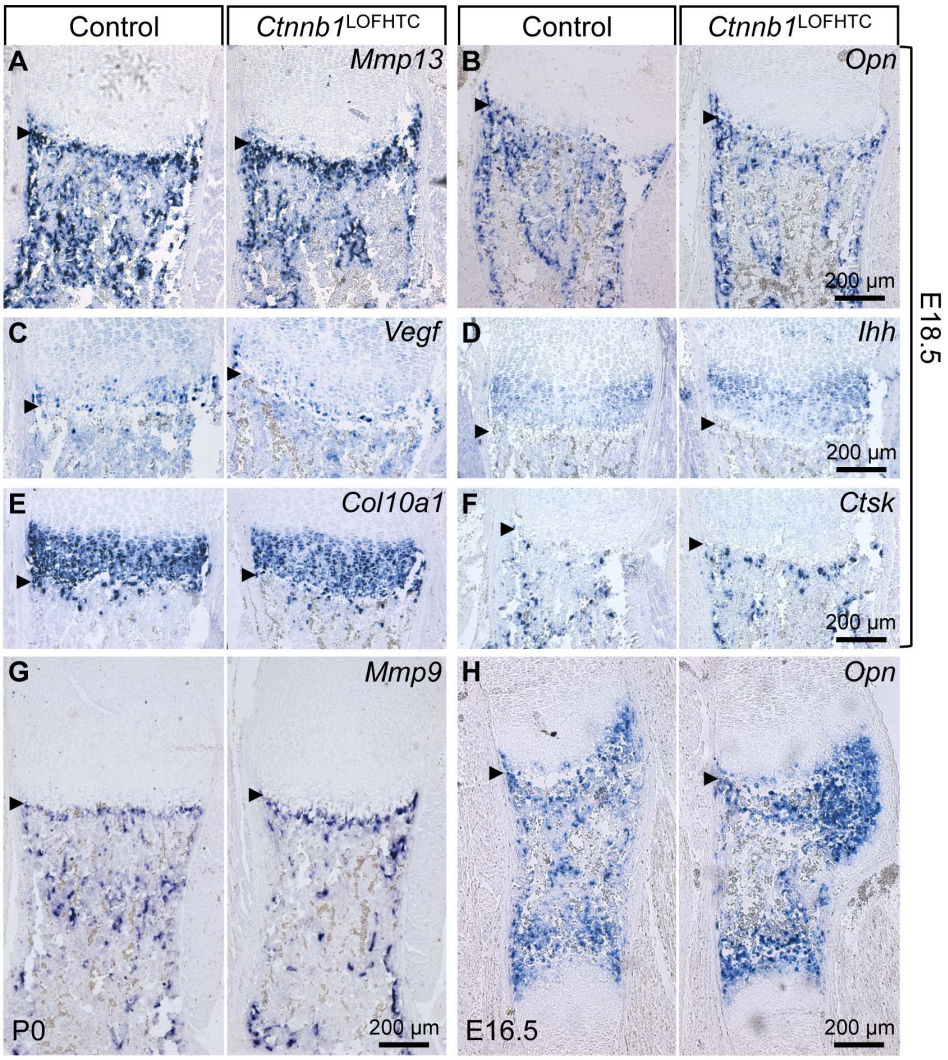

Fig. S1 Phenotypic analysis of *Ctnnb1*^{LOFHTC} mutants.
(A-F) Representative images of alternating sections through E18.5 humeri of control (*Ctnnb1*$^{fl/+}$;*Col10a1*-Cre^{-}) and *Ctnnb1*^{LOFHTC} (*Ctnnb1*$^{LacZ/fl}$;*Col10a1*-Cre^{+}) littermates. **(A)** In situ hybridization for *Mmp13* showing increased *Mmp13* signal at the chondro-osseous front and less staining in the region of the primary spongiosa in the mutant compared to the littermate control. **(B)** In situ hybridization for *Opn* showing a slight increase in *Opn* staining at the chondro-osseous front and less staining in the region of the primary spongiosa in the mutant compared to the littermate control. **(C)** In situ hybridization for *Vegf* showing no obvious difference between mutant and littermate control. **(D)** In situ hybridization for *Ihh* showing a slightly more intense signal in the mutant compared to the littermate control. **(E)** In situ hybridization for *Col10a1* showing no obvious difference between mutant and littermate control. **(F)** In situ hybridization for *Ctsk* reflecting an increase in osteoclasts at the chondro-osseous border in the mutant compared to the littermate control. **(G)** In situ hybridization for *Mmp9* on sections through P0 humeri showing a slight increase in *Mmp9* positive cells at the chondro-osseous front in the mutant compared to the littermate control. **(H)** In situ hybridization for *Opn* on sections through E16.5 humeri showing a slight increase in the signal at the chondro-osseous front in the mutant compared to the littermate control. The arrowhead marks the position of the chondro-osseous front.

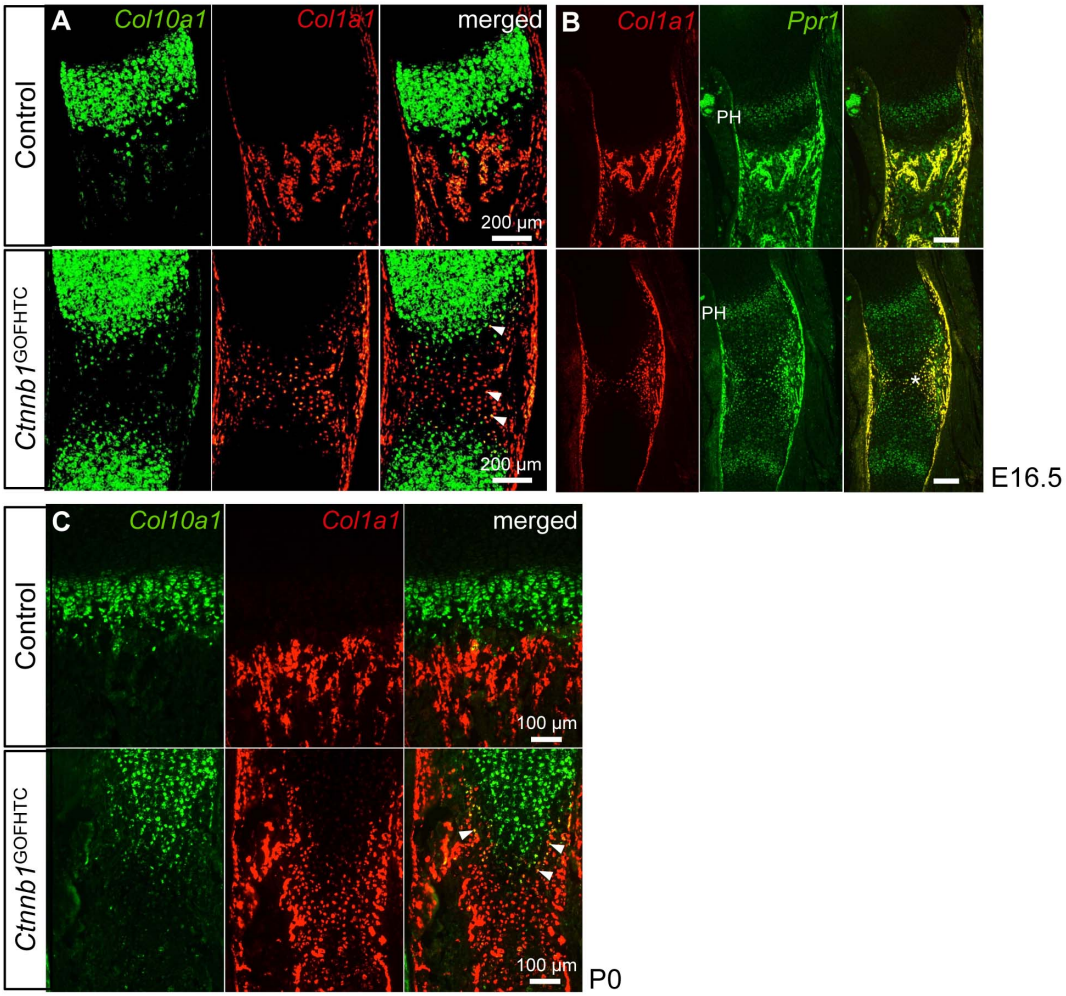

Fig. S2 Extended phenotypic analysis of *Ctnnb1*^{GOFHTC} mutants

(A-C) Double fluorescent in situ hybridization for *Col10a1*, *Col1a1*, and *Ppr1* on E16.5 (A,B) and P0 (C) humeri of control (*Ctnnb1*$^{ex3fl/+}$;*Col10a1*-Cre^{-}) and *Ctnnb1*^{GOFHTC} (*Ctnnb1*$^{ex3fl/+}$;*Col10a1*-Cre^{+}) specimens. Single channels and merged images are shown. **(A)** The signals for *Col10a1* (green) and *Col1a1* (red) are restricted to the HTC zone and the bone collar / trabecular bone, respectively in the control, while *Col1a1* positive cells are also found in the central most chondrogenic region of the *Ctnnb1*^{GOFHTC} humerus. Note: the *Col10a1* and the *Col1a1* signals in the chondrogenic regions hardly overlap - only a few yellow cells can be seen (white arrow heads). **(B)** The signals for *Col1a1* (red) and *Ppr1* (green) overlap in the control in the bone collar and trabecular bone. In the *Ctnnb1*^{GOFHTC} mutant, the signals also overlap in the central most chondrogenic region (asterisk). Ppr1 is also expressed in prehypertrophic chondrocytes (PH). **(C)** Double fluorescent in situ hybridization for *Col10a1* and *Col1a1* on P0 humeri, confirming the minimal coexpression of the two markers at the transition from *Col10a1* to *Col1a1* positive cells in the central chondrogenic region in the *Ctnnb1*^{GOFHTC} specimens.

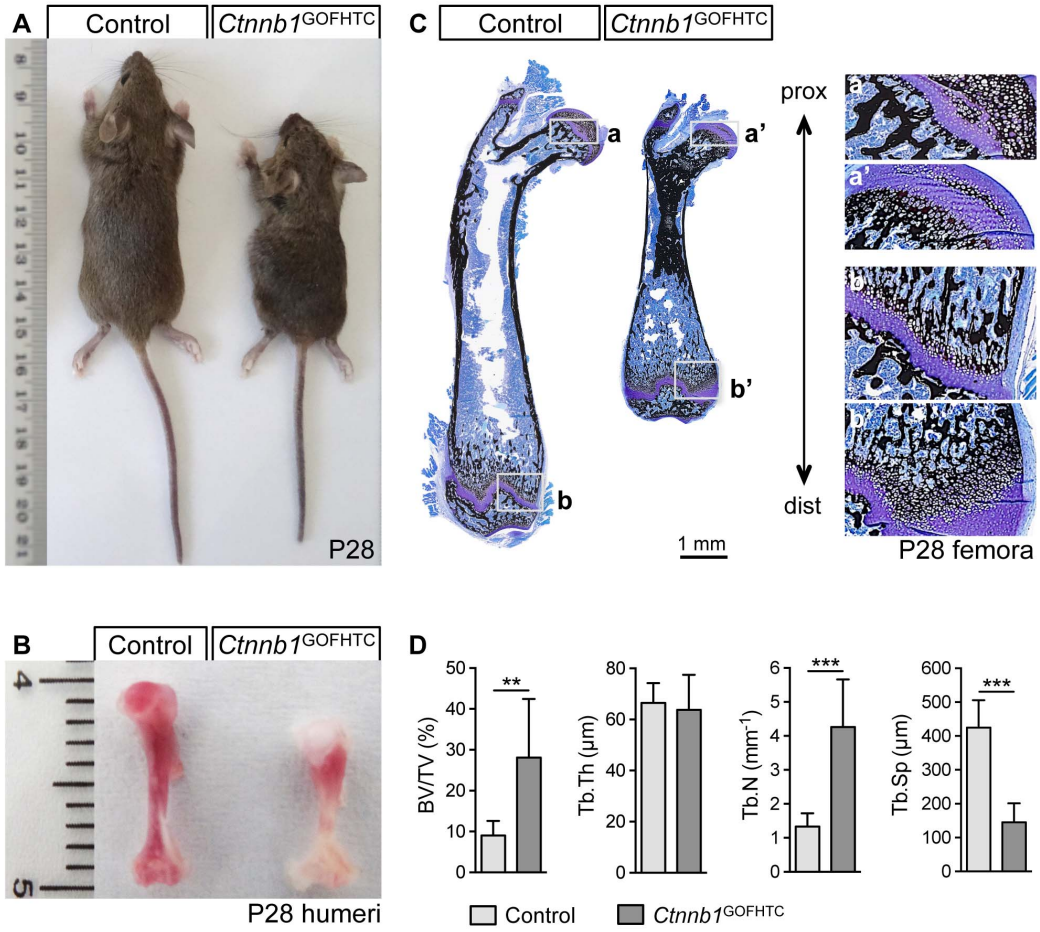

Fig. S3 Phenotypic characterization of *Ctnnb1*^{GOFHTC} at postnatal stage P28.
(A) *Ctnnb1*^{GOFHTC} mutant mice are smaller than their control (*Ctnnb1*$^{ex3fl/+}$;*Col10a1*-Cre^{-}) littermates. **(B)** Image of a humerus showing a reduction in the overall length and partial loss of hematopoiesis in the mutant compared to the humerus from the littermate control. **(C)** Composite toluidine blue / von Kossa stained images showing sections through P28 femora of *Ctnnb1*^{GOFHTC} and control littermates. In the mutant, there is an abnormal dense mineralized structure visible in the proximal region. (**a-b'**) show higher magnification of the boxed proximal and distal growth plate regions revealing an expansion of the mineralized hypertrophic region in the mutant (a', b') compared to the littermate control (a, b). **(D)** Histomorphometric quantification of the bone volume (BV) to total volume (TV), trabecular thickness (Tb. Th), trabecular number (Tb. N) and trabecular spacing (Tb. Sp) of P28 distal femora regions comparing *Ctnnb1*^{GOFHTC} (n=8) and littermate controls (n=9). **P-value < 0.01, ***P-value < 0.001, ± s.d.

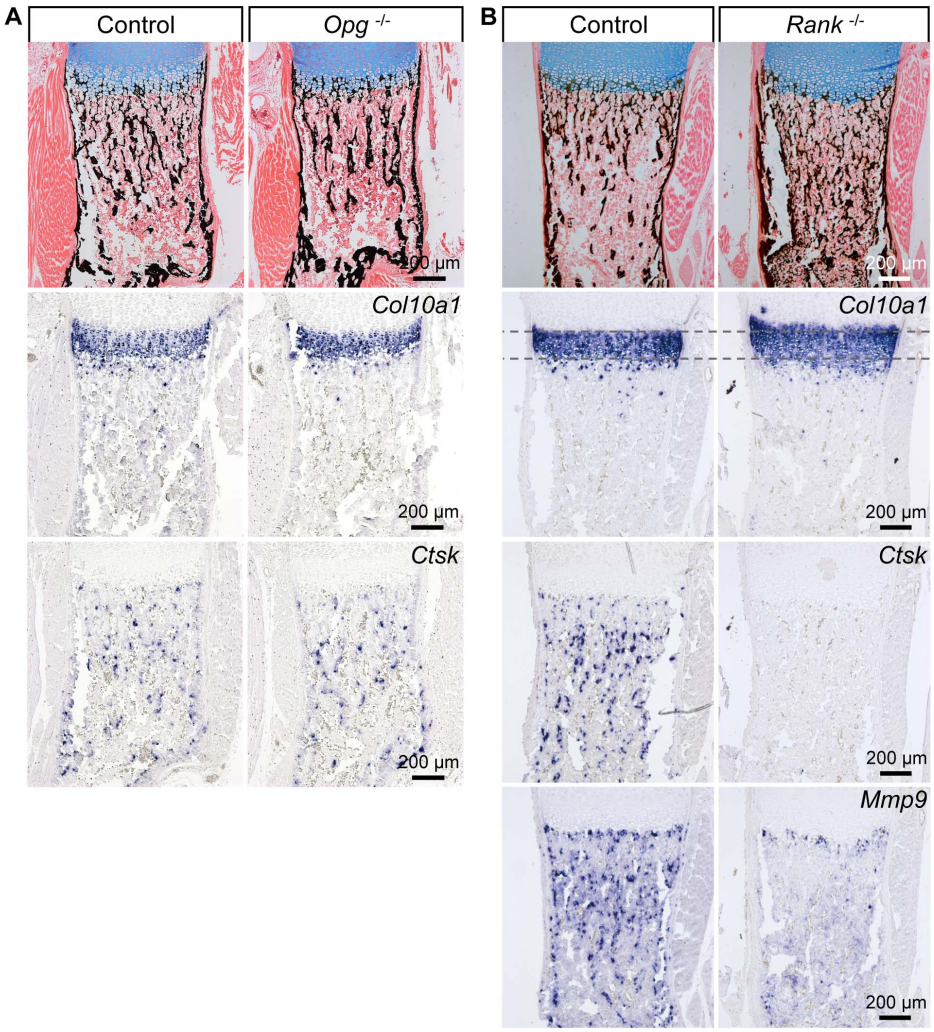

Fig. S4 Characterization of the *Opg* and *Rank*-deficient specimens.
(**A**) Histological and marker analysis on sections through P0 humeri of *Opg* mutants and littermate controls (*Opg*$^{+/+}$): showing a slight reduction in trabecular bone formation compared to the wild type control visualized by von Kossa staining, no difference in the width of the hypertrophic zone visualized by the *Col10a1* in situ hybridization, and no obvious increase in osteoclasts visualized by *Ctsk* in situ hybridization. (**B**) Histological and marker analysis on sections through P0 humeri of germ line deleted *Rank* mutants and littermate controls (*Rank*$^{+/+}$): showing an increase in mineralized structures particularly in the diaphysis compared to the wild type control visualized by the von Kossa staining. *Col10a1* in situ hybridization revealed an increased width of the hypertrophic zone in the mutant compared to wild type littermate. Osteoclasts were completely absent based on the *Ctsk* in situ hybridization while *Mmp9* positive cells are still present and primarily localized at the chondro-osseous junction.

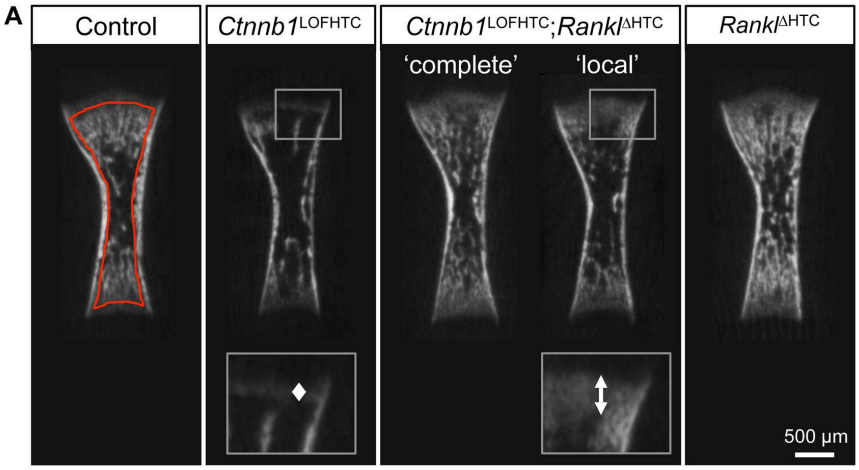

B

BV/TV (%)				
Control	*Ctnnb1*^{LOFHTC}	*Ctnnb1*^{LOFHTC};*Rankl*$^{\Delta HTC}$		*Rankl*$^{\Delta HTC}$
		'complete'	'local'	
45.90 ± 4.51	17.77 ± 4.06	39.56 ± 2.40	20.20 ± 1.87	61.16 ± 5.89

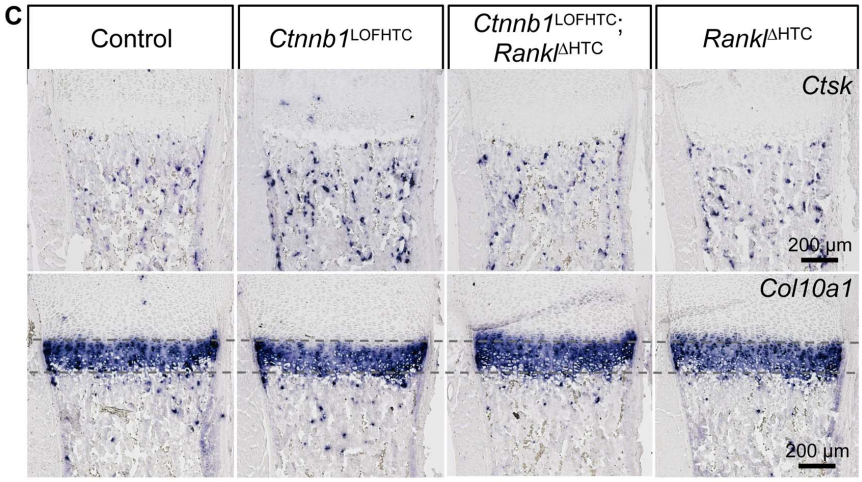

Fig. S5 Characterization of *Ctnnb1*^{LOFHTC};*Rankl*$^{\Delta HTC}$ specimens.
(A) Representative microCT images of humeri from control, *Ctnnb1*^{LOFHTC} (*Ctnnb1*$^{LacZ/fl}$;*Col10a1*-Cre^{+}), *Ctnnb1*^{LOFHTC};*Rankl*$^{\Delta HTC}$ ('complete' and 'locally' restored) (*Ctnnb1*$^{LacZ/fl}$;*Rankl* $^{fl/fl}$;*Col10a1*-Cre^{+}), and *Rankl*$^{\Delta HTC}$ (*Rankl*$^{fl/fl}$;*Col10a1*-Cre^{+}) specimens. The red line shown in the control humerus outlines the quantified area in an exemplary manner. Note: the 'locally restored' *Ctnnb1*^{LOFHTC};*Rankl*$^{\Delta HTC}$ specimen show only a local increase in the width of the dense area right around the chondro-osseous junction compared to the *Ctnnb1*^{LOFHTC} specimen (indicated by the double arrow in the insets). (**B**) Table showing the mean values of the BV/TV in % of control, *Ctnnb1*^{LOFHTC}, *Ctnnb1*^{LOFHTC};*Rankl*$^{\Delta HTC}$ ('complete' and 'local'), and *Rankl*$^{\Delta HTC}$ specimens (± s.d.), on which the dot plot shown in Fig. 5A is based. (**C**) Representative images of sections through humeri of control, *Ctnnb1*^{LOFHTC}, *Ctnnb1*^{LOFHTC};*Rankl*$^{\Delta HTC}$ ('complete'), and *Rankl*$^{\Delta HTC}$ specimens, hybridized with *Ctsk* and *Col10a1* probes showing that the increase in *Ctsk* positive cells in the *Ctnnb1*^{LOFHTC} mutant is corrected by the additional loss of *Rankl* in HTCs in the Rescue$^{\Delta Rankl}$ specimens. Note: no obvious differences in the number of *Ctsk* positive cells are visible comparing the *Rankl*$^{\Delta HTC}$ mutants with control. The width of the HTC zone is not significantly altered in any of the mutants compared to the control (*Ctnnb1*$^{fl/+}$;*Col10a1*-Cre^{-}).

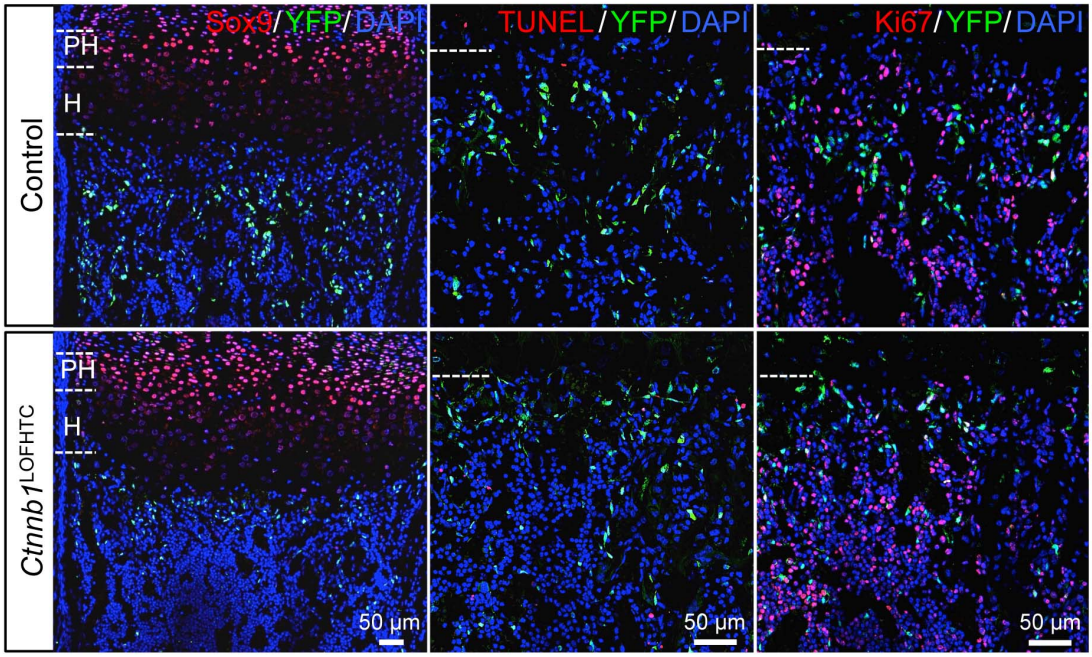

Fig. S6 Effects of the loss of *Ctnnb1* in HTCs on chondrocyte-derived osteoblastogenesis.

Representative fluorescent images of control and *Ctnnb1*^{LOFHTC} P0 proximal growth plates triple-stained for Sox9/YFP/DAPI on the left, TUNEL/YFP/DAPI in the middle, and Ki67/YFP/DAPI on the right. PH: prehypertrophic zone, H: hypertrophic zone. The dashed lines in the middle and right images indicate the position of the chondro-osseous front. Genotypes: control = *Ctnnb1*$^{fl/+}$;*Col10a1*-Cre^{+};*Rosa26*$^{YFP/+}$, *Ctnnb1*^{LOFHTC} = *Ctnnb1*$^{LacZ/fl}$;*Col10a1*-Cre^{+};*Rosa26*$^{YFP/+}$.

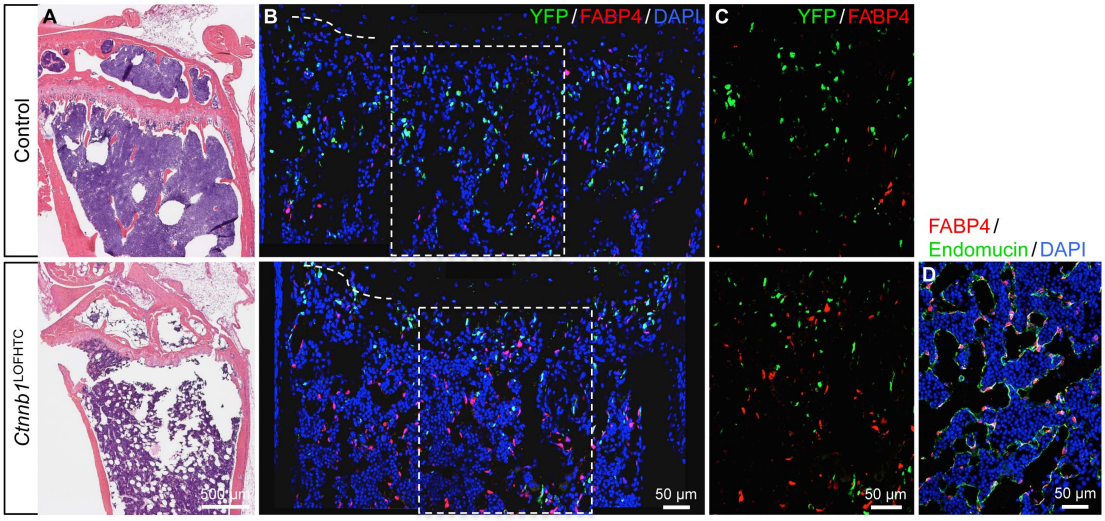

Fig. S7 Increased adipogenesis in *Ctnnb1*^{LOFHTC} mutants

(**A**) Images of H&E stained sections of four-month-old control (*Ctnnb1*$^{fl/+}$;Col10a1-Cre^{-}) and *Ctnnb1*^{LOFHTC} femora showing an increase in adipocytes in the bone marrow of the mutant (whitish, round cells). (**B**) Representative composites of three images each of control (*Ctnnb1*$^{fl/+}$;*Col10a1*-Cre^{+};*Rosa26*$^{YFP/+}$) and *Ctnnb1*^{LOFHTC} (*Ctnnb1*$^{LacZ/fl}$;*Col10a1*-Cre^{+};*Rosa26*$^{YFP/+}$) P0 specimens taken from the region below the chondro-osseous front. Immunofluorescent staining for FABP4 (red), YFP (green), and DAPI for nuclei (blue), showing an increase in cells that are positive for FABP4 but negative for YFP in the *Ctnnb1*^{LOFHTC} primary spongiosa. The dashed line indicates the position of the chondro-

osseous border. (**C**) Higher magnification images of the boxed regions in (B) with only the FABP4 (red) and YFP (green) signals shown. Note: There are no yellow $FABP4^{+};YFP^{+}$ cells visible. (**D**) Immunofluorescent staining for FABP4 (red), endomucin (green), and DAPI (blue) showing that the FABP4-positive cells are closely associated with endomucin-positive blood vessels.